Both Constitutive and Inducible Prostaglandin H Synthase Affect Dermal Wound Healing in Mice

Stanley J. F. Laulederkind, Sandra Thompson-Jaeger, Sarita Goorha,
Qingshan Chen, Amina Fu, Jae-Young Rho, Leslie R. Ballou, and Rajendra Raghow

Department of Veterans Affairs Medical Center (SJFL, ST-J, SG, AF, LRB, RR), the Department of Biomedical Engineering (QC, J-YR), University of Memphis, and the Departments of Molecular Sciences (LRB), Medicine (LRB), and Pharmacology (SJFL, RR), University of Tennessee Health Sciences Center, Memphis, Tennessee

SUMMARY: In an attempt to define the roles of prostaglandin H synthase 1 (PGHS-1, cyclooxygenase-1, COX-1) and prostaglandin H synthase 2 (PGHS-2, cyclooxygenase-2, COX-2) in wound healing, we investigated the healing of incisional dermal wounds in wild-type, PGHS-1 null, and PGHS-2 null mice. We measured tensile strength of the wounds, levels of PGHS-1 and PGHS-2 mRNA in the wound site, and histologic markers for the inflammatory, proliferative, and remodeling phases of wound healing. Although no gross visible differences were noted among healed wounds of the different mouse types, measurement of tensile strength showed that both PGHS-1 and PGHS-2 null wounds were weaker (75% and 70%, respectively) than wild-type wounds at 12 days after incision. At Day 8 the endothelial staining was 70% greater in the wounds of PGHS-2 null mice compared with their wild-type counterparts. In contrast at Day 12, staining for macrophages and myofibroblasts was less in PGHS-1 null wounds compared with wild-type and PGHS-2 null tissue. Compensatory expression of the alternate PGHS mRNA could be demonstrated by RT-PCR in the wounds of PGHS null mice on Days 1 and 4. We conclude that both PGHS-1 and PGHS-2 genes play distinct roles in the process of dermal wound healing. (*Lab Invest 2002, 82:919–927*).

The incisional wound healing response in mammals begins with hemostasis and is followed by inflammatory, proliferative, and remodeling phases (Martinez-Hernandez, 1996; Mast, 1992; Raghow, 1994; Schilling, 1976). Prostaglandin E_2 (PGE_2) and prostaglandin I_2 are proinflammatory mediators involved during the acute inflammatory phase (Schumacher, 1988). These two prostaglandins are potent vasodilators that also act synergistically with other mediators to increase microvascular permeability. PGE_2 is also involved in the proliferative phase of wound healing, by stimulating fibroblast mitogenesis (Castano et al, 2000; Moreno, 1997, 2000). Thromboxane A_2 is another prostanoid possibly important in wound healing because of its ability to stimulate endothelial migration (Daniel et al, 1999; Nie et al, 2000). Prostaglandin H synthase (PGHS, cyclooxygenase, COX) catalyzes the committed step in prostaglandin and thromboxane biosynthesis. Through the action of prostanoids, PGHS isozymes (the constitutive isozyme PGHS-1 or the inducible isozyme PGHS-2) contribute to the processes of inflammation, cellular proliferation (Smith and Langenbach, 2001), and neovascularization (Tsujii et al, 1998).

The presence of PGE_2 or active PGHS enzyme has been reported to be beneficial to the healing process in various models of tissue repair (Brzozowski et al, 1993; Fang et al, 1983; Gonul et al, 1993; LeDuc et al, 1993). This has been demonstrated by exogenously adding the stable PGE_2 analog 16,16-dimethyl prostaglandin E_2-methyl ester (Brzozowski et al, 1993), PGHS inhibitors (Brzozowski et al, 1993; Dong et al, 1993; Fang et al, 1983; LeDuc et al, 1993; Sun et al, 2000), or agents that increase plasma PGE_2 levels (Gonul et al, 1993). There is some evidence to suggest that PGE_2 may be more important in the early stages of wound healing, causing increased fibrosis and decreased accumulation of macrophages by 7 days after injury (Talwar et al, 1996). In vitro models of wound healing also show a role for PGE_2, because it may be involved in the platelet-derived growth factor–mediated signals that cause proliferation of fibroblasts (Sanchez and Moreno, 2001).

The development of PGHS null mice (Dinchuk et al, 1995; Langenbach et al, 1995; Morham et al, 1995) has presented the opportunity to investigate the individual roles of PGHS-1 and PGHS-2 in wound healing. By using mice lacking either PGHS-1 or -2, we sought to determine which isozyme is more important for producing those lipid mediators that provide signals for the inflammatory, proliferative, and angiogenic processes involved in dermal wound healing. We analyzed full-thickness incisional wounds of the skin by tensile strength measurements and immunohisto-

chemistry. Our data suggested that PGHS-1 and PGHS-2 affected different aspects of dermal wound healing, yet tensile strength of wounds was affected adversely by the lack of either isozyme.

Results

Tensile Strength Measurements of Incisional Dermal Wounds of Wild-Type, PGHS-1 Null, and PGHS-2 Null Mice

Prostanoids, downstream products of PGHS-1 and -2, are important for inflammation, fibroblast proliferation, and angiogenesis, all of which are involved in wound healing. To determine whether PGHS-1 and -2 play unique roles in wound healing and tissue regeneration, we used a model of incisional wound healing using wild-type, PGHS-1 null, and PGHS-2 null mice. We made similar dermal incisions in all mouse types and allowed healing to occur for various times up to 12 days. Superficial examination of incisional wounds showed nearly complete healing in all three types of mice by 12 days after incision. There were no discernible differences among the external appearance of healed wounds of PGHS-1 null, PGHS-2 null, and wild-type mice at any time point during the healing process. Therefore to determine any functional differences among the wounds of the three types of mice, we tested the tensile strength of wounds.

To determine the breaking strength of healed wounds, we killed animals 12 days after wounding and removed skin samples for tensile strength measurements. Multiple strips of skin were cut from the wound site and subjected to increasing bilateral stretching until the skin broke along the axis of incision. The tensile strength of 12-day-old wounds showed statistically significant differences between wild-type and PGHS null mice. The strength of the healed wild-type skin was about 1.3 times greater than that of PGHS-1 null mice and about 1.5 times greater than that of PGHS-2 null mice (Fig. 1). The decreases in wound strength were significant based on Student's t tests ($p < 0.0001$ for PGHS-1 and $p < 0.001$ for PGHS-2).

Histologic Analysis of Dermal Wound Sites from Wild-Type, PGHS-1 Null, and PGHS-2 Null Mice

The observation that wound strength was lessened in the absence of PGHS-1 or PGHS-2 suggested an alteration in one or more processes involved in repair of injured tissue in the PGHS null mice. Therefore, we examined the temporal expression of a number of key marker molecules by immunohistochemistry, to assess alterations in neutrophil and macrophage infiltration, endothelial cell proliferation, angiogenesis, and proliferation of myofibroblasts. Because the inflammatory phase of wound healing in the first 24 hours is characterized by infiltration of neutrophils, we assessed the rates of neutrophil migration between 2 and 24 hours after the incision. We saw a rise in neutrophil infiltration in all three types of mice until 16 hours after incision; the neutrophil infiltration plateaued in all wounds after 16 hours (Fig. 2). The only
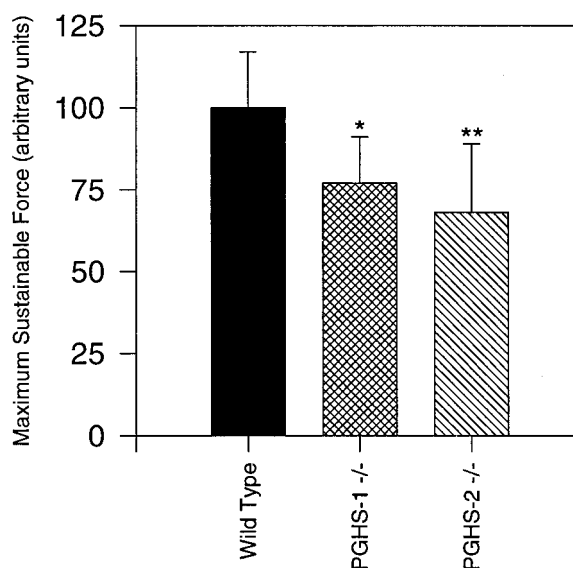

Figure 1.

Tensile strength of wounds after 12 days of healing. The maximum sustainable force in newtons was determined for each excised wound from wild-type (n = 12), prostaglandin H synthase 1 (PGHS-1) null (n = 9), and prostaglandin H synthase 2 (PGHS-2) null (n = 8) mice. The graph values are averages from four separate experiments and represent percentage of wild-type wound strength. Statistics were calculated with Student's t tests (*$p < 0.0001$ and **$p < 0.001$).
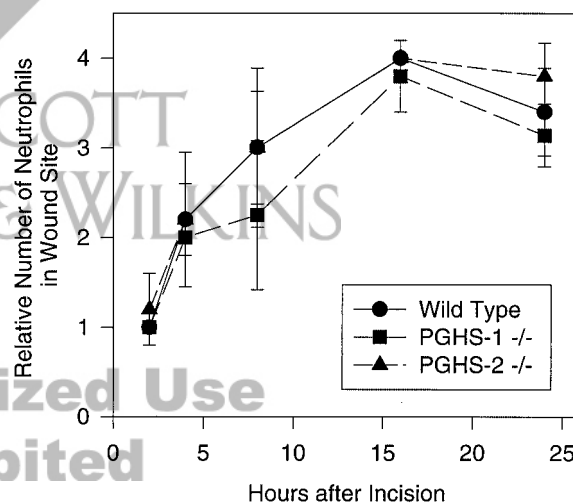

Figure 2.

Time course of neutrophil infiltration of wound site during first 24 hours of healing. Relative numbers of neutrophils were determined by blinded grading of histologic sections (6-μm sections stained with hematoxylin and eosin). Each time point represents five to seven animals.

difference among mouse types was observed at 8 hours. Compared with wild-type mice, the PGHS-1 null mice displayed a lag in neutrophil migration, which recovered to normal by 16 hours. However, the differences were not statistically significant ($p < 0.2$).

At a number of time points between 24 hours and 12 days after incisions, tissue sections were stained for endothelial cell, macrophage, and myofibroblast markers. As with the neutrophil infiltration, PGHS null mice showed minor changes in staining compared with wild-type mice.

The marker used for endothelial cells was von Willebrand factor. The staining showed minor changes at Day 4 for PGHS-2 null mice and at Day 8 for both PGHS-1 and PGHS-2 null mice (Figs. 3 and 4). The staining for endothelial cells was greater in PGHS-2 null tissue. The 30% increase in endothelial cell staining seen at 4 days ($p < 0.5$) in PGHS-2 null tissue was not significant; but the 70% increase in staining observed in Day 8 wounds was significant ($p < 0.03$).

The marker used for macrophages was α-1-antitrypsin. A statistically significant difference was found at Day 12 in the PGHS-1 null mice ($p < 0.01$). At a point when the macrophage population was disappearing in the healing wound sites of all mice, the tissues of PGHS-1 null mice showed a steeper rate of decline in macrophage numbers compared with both wild-type and PGHS-2 null tissue (Figs. 5 and 6).

Staining of smooth muscle actin was used as a marker of myofibroblasts. These cells are considered to be important for wound contraction as well as known for playing a role in production of extracellular matrix molecules (Zhang et al, 1994). Again, small differences were observed between wild-type mice and both PGHS-1 and -2 null mice (Fig. 7). These differences were not statistically significant.

RT-PCR Analysis of Total RNA Extracted from Dermal Wound Sites from Wild-Type, PGHS-1 Null, and PGHS-2 Null Mice

To correlate expression of PGHS-1 and PGHS-2 with changes in immunohistochemistry among the three types of mice, we extracted RNA from dermal wound sites at Days 1, 4, 8, and 12 after incision and analyzed the abundance of PGHS-1 and PGHS-2 mRNA. A representative gel electrophoresis pattern of competitive RT-PCR products from various wound samples is shown in Figure 8. In the wounds of PGHS-1 null mice, the compensatory induction of PGHS-2 mRNA at Days 1 and 4 is clearly visible (Fig. 8B). In contrast, the compensatory induction of PGHS-1 mRNA in PGHS-2 null tissue was much lower at Day 1 and insignificant at Day 4 (Fig. 8A). There is no compensatory steady-state accumulation of mRNAs encoding either isozyme at Day 8; the degree of compensation by either isozyme at Day 12 is also much smaller compared with that seen at earlier time points (Fig. 8). In the wild-type mice, expression of PGHS-1 mRNA decreased noticeably between Days 8 and 12. The absence of PGHS-2 mRNA in the wounds at 12 days correlates well with the immunohistochemical staining; there were no discernible differences in the staining for any of the cellular markers between wild-type and PGHS-2 null animals at 12 days. The continued expression of PGHS-1 mRNA at 12 days in the wounds of wild-type mice is consistent with the differences seen at 12 days between wild-type and PGHS-1 null mice wounds stained for α1-antitrypsin and smooth muscle actin, markers for macrophages and myofibroblasts, respectively.

Discussion

Dermal wound healing is a complex process involving phases of hemostasis, inflammation, cellular proliferation, and tissue remodeling (Martinez-Hernandez, 1996; Mast, 1992; Raghow, 1994; Schilling, 1976). The role of prostaglandins in wound healing has previously been studied by using PGHS inhibitors (Brzozowski et al, 1993; LeDuc et al, 1993), by using exogenously added prostaglandin (Brzozowski et al, 1993), or by exogenously inducing the synthesis of prostaglandins (Gonul et al, 1993). These studies indicated that cyclooxygenases and their downstream products, prostaglandins, were involved in dermal wound healing. However, the roles of individual PGHS-1 and PGHS-2 isozymes remained obscure. In this study we have sought to determine the relative contributions of PGHS-1 and PGHS-2 to the healing of incisional dermal wounds using PGHS-1 and PGHS-2 null mice.

The overall impact of PGHS-1 and PGHS-2 on dermal wound healing was assessed by measurements of tensile strength. The healed wounds of both PGHS-1 null and PGHS-2 null animals were weaker than those of wild-type mice. Although the differences in tensile strengths of wounds among wild-type, PGHS-1 null, and PGHS-2 null mice were moderate, they were statistically significant. This indicated that both isozymes participated in the process of normal wound healing of dermal incisions.

The assessment of healing wounds by immunohistochemical markers for various cellular components revealed only minor changes at a few different time points. No statistically significant differences were seen in the distribution of any particular cell type from 2 hours to 4 days after incision. However, the evaluation of the steady-state levels of mRNAs by a competitive RT-PCR method suggested that PGHS-1 had a larger role than PGHS-2 at Days 1 and 4 after incision. In the PGHS-1 null tissue, the expression of PGHS-2 mRNA was much greater than that of PGHS-1 mRNA in the PGHS-2 null wounds. These data suggest that the lack of one PGHS isozyme leads to compensatory expression of the remaining gene, and the degree of such compensation seems to be variable.

At 8 days after incision, endothelial cell staining was greater in both PGHS-1 and PGHS-2 null mice than in wild-type mice. However, by Day 12 there were no differences between the PGHS null mice and wild-type endothelial cell staining. Therefore, the lower level of endothelial staining and vessel formation in wild-type mice at Day 8 seemed to be of no lasting consequence.

PGHS-1 seemed to be more important than PGHS-2 in generating signals for sustained attraction of macrophages, as judged by immunohistochemistry. This conclusion was supported by the RT-PCR data from wild-type mice that showed continued presence of PGHS-1 in the 12-day wounds, whereas PGHS-2 mRNA disappeared by Day 12. There was a low level of compensatory accumulation of both mRNAs in the PGHS null animals, with relative amounts of PGHS-1
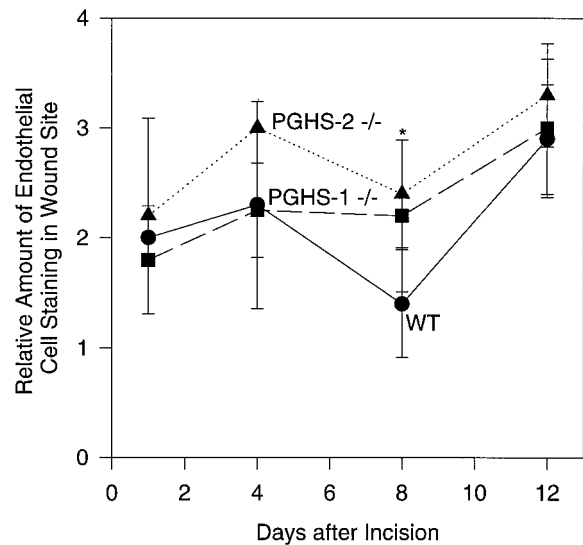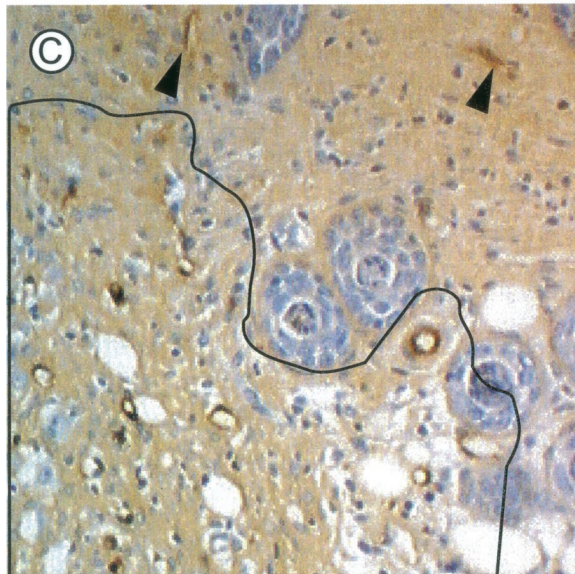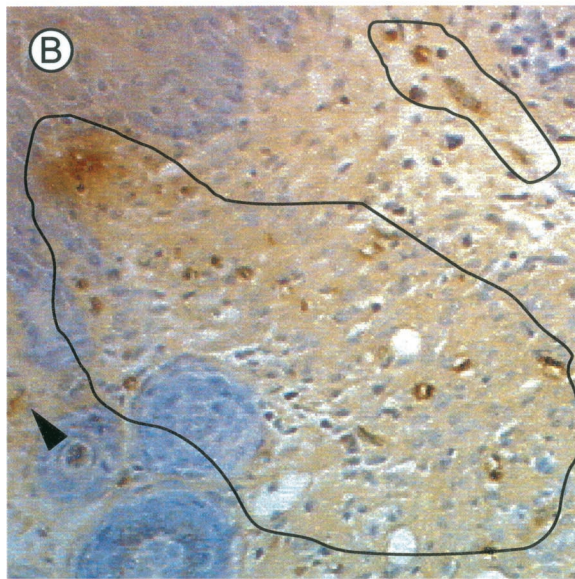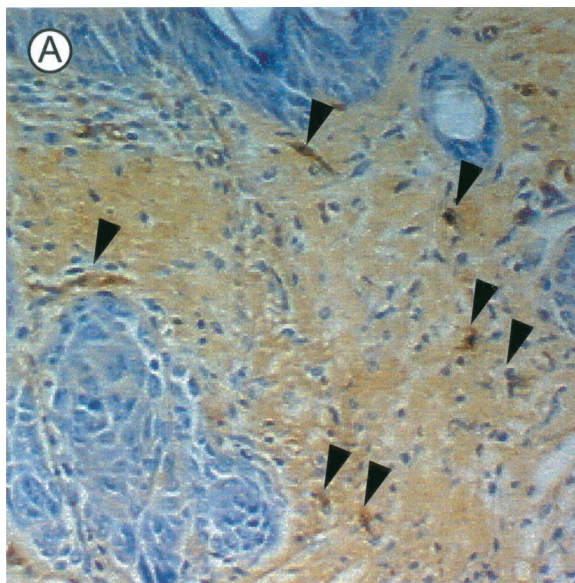
Figure 4.

Time course of endothelial staining in wound site during first 12 days of healing. Relative extent of staining was determined by blinded grading of histologic sections (6-μm sections stained by immunohistochemistry for von Willebrand's factor). Each time point represents five to six mice. Statistics were calculated with Student's *t* tests (*$p < 0.03$).

and -2 reflecting their relative steady-state levels in the wounds of wild-type mice. Myofibroblast staining was lower in PGHS-1 null animals than in wild-type or PGHS-2 animals on both Days 8 and 12. This again suggested the greater importance of PGHS-1 in healing during the second week after incision. Published data support the importance of prostaglandins in myofibroblast growth, because PGE_2 enhances epidermal growth factor-stimulated and fibroblast growth factor-2-stimulated proliferation of myofibroblasts in culture (Boyle et al, 1999), and indomethacin was shown to inhibit myofibroblast proliferation in the healing gastric ulcers (Hirose et al, 1997).

Based on the data presented here we suggest that both PGHS-1 and PGHS-2 are needed for optimal healing of dermal wounds. The unique contribution of the two PGHS isozymes is underscored by expression of the alternate gene to compensate for the deficit in the PGHS-1 and PGHS-2 null mice. The compensatory production of the remaining PGHS isozyme in the wounds of PGHS-1 and PGHS-2 null mice corroborates our previous observations (Kirtikara et al, 1998; Zhang et al, 2002) showing that PGHS isozyme compensation varies widely from one tissue to another and in response to different experimental conditions.

Figure 3.

Wound site after 8 days of healing in wild-type (*top panel*), PGHS-1 null (*center panel*), and PGHS-2 null (*bottom panel*) mice. The 20× sections were stained by immunohistochemistry for von Willebrand's factor. The dark brown staining (*arrowheads* and *areas enclosed by black lines*) indicates endothelial cells, many of which outline the lumen of blood vessels, especially in the PGHS null mice. These sections are representative of five to six animals.
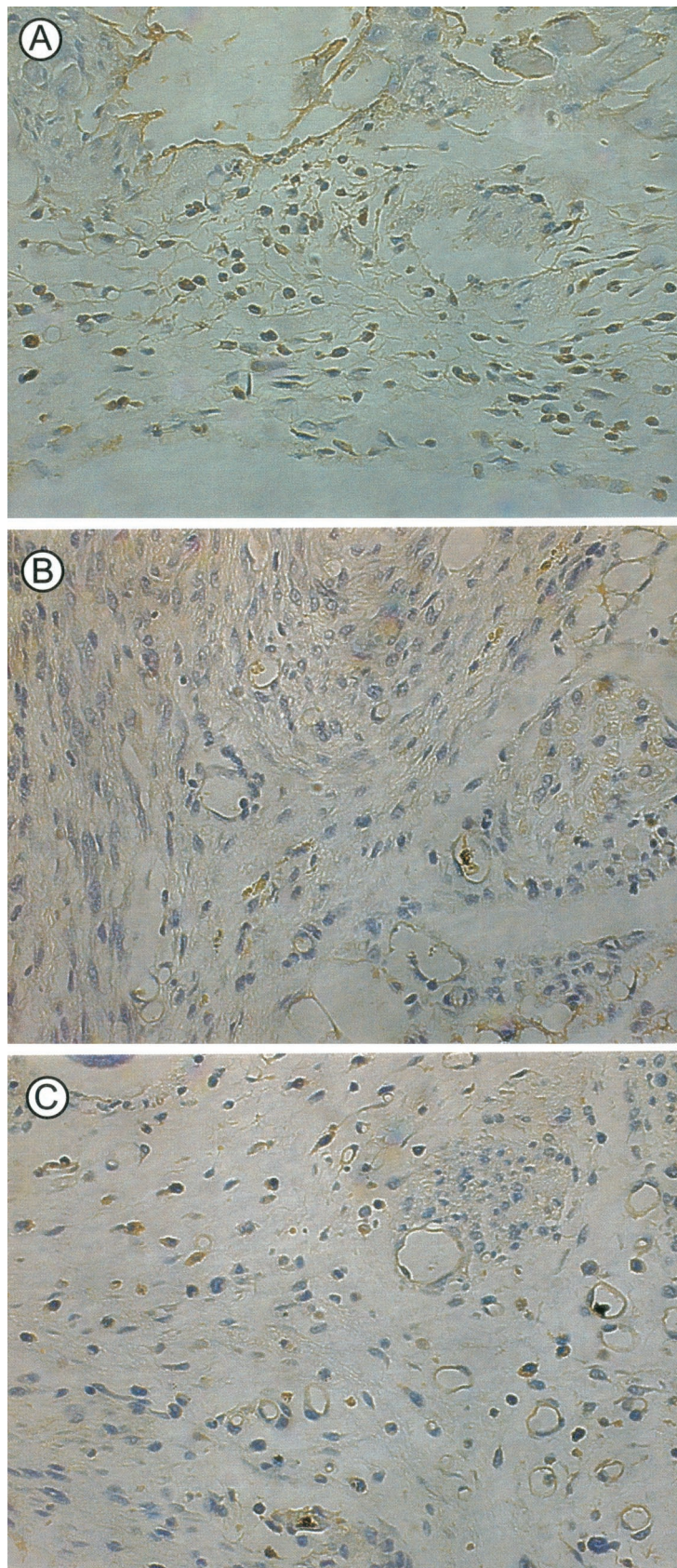
Figure 5.
Wound site after 12 days of healing in wild-type (*top panel*), PGHS-1 null (*center panel*), and PGHS-2 null (*bottom panel*) mice. The 40× sections were stained by immunohistochemistry for α1-antitrypsin. The dark brown staining of individual cells is specific for macrophages. Each of these images is representative of five to six animals.
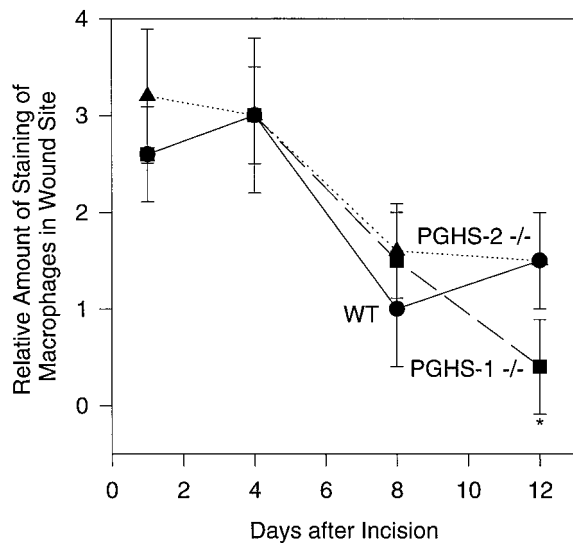
Figure 6.

Time course of macrophage trafficking in wound site during first 12 days of healing. Relative numbers of macrophages were determined by blinded grading of histologic sections (6-μm sections stained by immunohistochemistry for α1-antitrypsin). Each time point represents five to six animals. Statistics were calculated with Student's *t* tests (*$p < 0.01$).
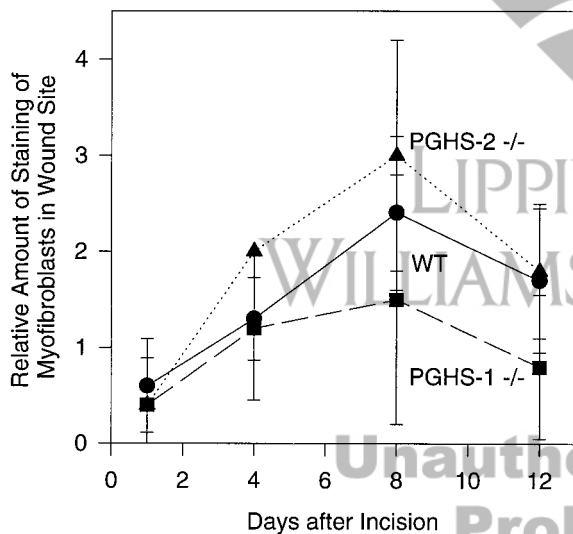

Figure 7.

Time course of myofibroblast staining in wound site during first 12 days of healing. Relative extent of staining was determined by blinded grading of histologic sections (6-μm sections stained by immunohistochemistry for smooth muscle actin). Each time point represents five to six animals.

Materials and Methods

Animals

Strain C57/DBA1 of wild-type, PGHS-1 null, and PGHS-2 null mice used in these studies were developed at the Department of Veterans Affairs Medical Center in Memphis (Ballou et al, 2000) from mating pairs that originated at the University of North Carolina (Langenbach et al, 1995; Morham et al, 1995). Before experiments, animals were housed in Plexiglas cages at 25° C and kept on a 12-hour light/12 hour dark cycle in a virus-free environment. Food and water were available ad libitum. All experimental mice were 9 to 12 weeks of age. Because of fertility problems of the PGHS null mice, homozygous males were bred with heterozygous females to obtain the homozygous female mice used in all experiments. The genotypes of the animals were determined by PCR (Ballou et al, 2000).

Genotyping

DNA from tails was extracted by using the DNeasy Tissues Kit from Qiagen (Valencia, California). Tail samples were lysed overnight in a buffer containing proteinase K and loaded onto a minicolumn. After the column was washed, DNA was eluted in water or a buffer, ready for PCR. Three primers were used in the same PCR reactions for identification of the PGHS-1 or -2 allele. The wild-type allele 5' primer (PGHS1-5') AGGAGATGGCTGCTGAGTTGG, the mutant allele 5' primer (PGHS1-neo) GCAGCCTCTGTTCCACATA-CAC, and the 3' primer (PGHS1-3') AATCTGACTT-TCTGAGTTGCC were used to yield a fragment of 600 or 700 bp for the PGHS-1 wild-type or mutant allele, respectively. The wild-type allele 5' primer (PGHS2-5') ACACATCTATCACTGGCACC, the mutant allele 5' primer (NeoPro) ACGCGTCACCTTAATATGCG, and the 3' primer (TGC2-3) GTACGGCTTCAGGGAGAA yield a fragment of 600 or 800 bp for the PGHS-2 wild-type or mutant allele, respectively.

Incisional Wound Healing Model

Female mice, 9 to 12 weeks of age, were anesthetized by an ip injection of ketamine/xylazine (37.5 μg/37.5 μg per gm body weight). Additional inhalational anesthetic (methoxyflurane) was used as needed. First the hair was shaved off of the entire back of the mouse. A 1.5-cm anteroposterior full-thickness incision was then made on each side of the mouse's back. Each incision was closed with two sutures (4-0 silk). Each mouse was housed individually for the remainder of the experiment.

Tensile Strength Measurement

At 12 days after incision, mice were killed and wound site skin samples (2 $\times$ 2.5 cm) were collected. Several tissue strips 2 mm in width were cut from each sample using a specially designed cutter. The tissue strips were mounted in clamps in an Instron universal test machine with a small load cell (10 N) attached and stretched at a constant speed of 20 mm/minutes until failure. Both the force and elongation signals were digitized and captured on a personal computer. Maximum sustainable force in newtons was obtained from force-elongation curves generated for each test strip by LabView software.

Histology

At appropriate times, mice were killed and one wound site skin sample (15 $\times$ 15 mm) was collected, fixed in
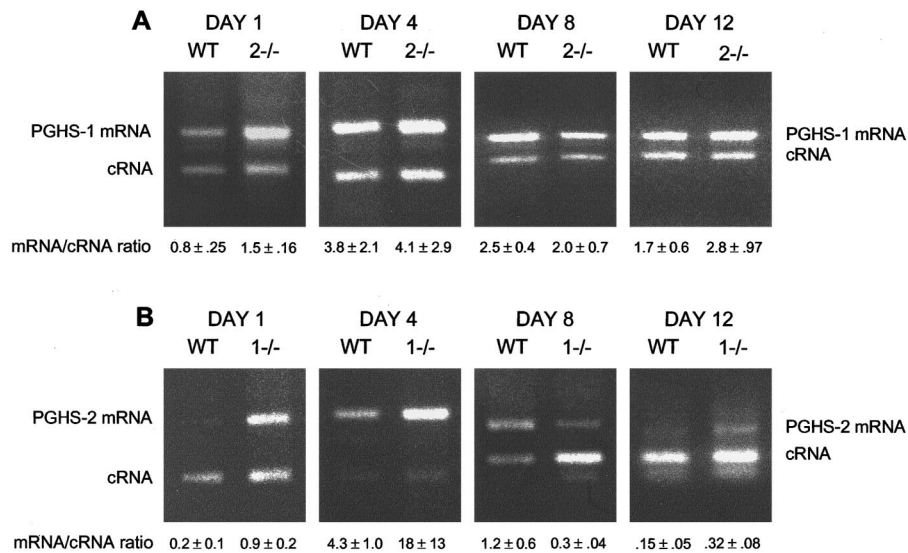
Figure 8.
Gel electrophoresis analysis of PGHS-1-specific and PGHS-2-specific RT-PCR products generated from RNA of wild-type, PGHS-1, and PGHS-2 null dermal wounds at 1, 4, 8, and 12 days after incision. PGHS-1-specific and PGHS-2-specific cRNAs were amplified as internal standards simultaneously with the corresponding mRNAs in the RT-PCR reactions, as described in "Materials and Methods." The ratios of mRNA/cRNA were determined from densitometric scans of the bands and calculated as the average values from two to three repeat reactions of three to four different samples for each time point. A, PGHS-1 mRNA/cRNA; B, PGHS-2 mRNA/cRNA.

10% buffered formalin, processed by graded dehydration, and embedded in paraffin for histologic analysis. For immunohistochemistry the slides were air-dried, dried in an oven for 15 minutes at 55° C to 60° C, deparaffinized, and hydrated. Immunoperoxidase staining was done on a Cadenza automated processor, using the appropriate primary antibody, biotinylated secondary antibody, horseradish peroxidase-conjugated streptavidin, and diaminobenzidine. Histology sections were graded on a scale of 0 to 4 by two blinded observers.

RNA Extraction from Wound Site Skin

A skin sample (~3 × 15 mm) from the second wound site from each dead animal was minced and homogenized in Trizol reagent (Sigma, St. Louis, Missouri). RNA was extracted from the homogenate. Briefly, a 20% volume of chloroform was added to the homogenate and shaken briskly. After a 15-minute centrifugation (12,000 ×g) to separate the aqueous and phenolic phases, the upper aqueous layer containing total RNA was removed to a clean tube. The RNA was precipitated by adding an equal amount of isopropanol, mixing, and centrifuging for 10 minutes at 12,000 ×g. The pellet was washed once with 75% ethanol and centrifuged as before. After air-drying, the RNA pellet was dissolved in sterile water and stored at −80° C.

RT-PCR Analysis of Wound Site RNA

Internal standards for RT-PCR of PGHS-1 and PGHS-2 were created as described elsewhere (Ballou et al, 2000) such that PCR products from cRNAs for PGHS-1 and PGHS-2 could be generated using the same deoxyoligonucleotide primers as for mRNAs in the RT-PCR reactions. The PGHS-1 cRNA product contained a 165-bp internal deletion (+1517 to +1681) of the PGHS-1 mRNA RT-PCR product (+1496 to +2097), and the PGHS-2 cRNA product contained a 131-bp internal deletion (+1351 to +1481) of the PGHS-2 mRNA RT-PCR product (+1227 to +1500).

First-strand cDNA was synthesized using Superscript II RNAse H-reverse transcriptase according to the manufacturer's instructions (Gibco-BRL, Gaithersburg, Maryland) with minor modification. Briefly, 1 μg of total sample RNA and cRNA internal standards were incubated with 50 ng of antisense oligonucleotide primers (PGHS-1: 5'-caaccagaaatctgactttctga-3'; PGHS-2: 5'-gtacggcttcagggagaa-3') for 90 minutes at 42° C. Pilot PCR of random samples from each time point determined the amount of cRNA internal standard added. In all cases equal amounts of cRNA internal standard were added to wild-type and PGHS null tissue from the same time point. The reverse transcription reaction was terminated by heating at 95° C for 10 minutes and followed by a brief centrifugation at room temperature. cDNA was cooled to room temperature and then stored at −20° C until further analysis.

cDNA samples were amplified by PCR using Ready-To-Go PCR Beads (Amersham Pharmacia Biotech, Inc., Piscataway, New Jersey) in a total volume of 25 μl. To keep reactions within the linear range of DNA amplification, PCR was performed for 30 cycles (94° C, 15 seconds; 60° C, 15 seconds; 72° C, 1 minute, 7 minutes for the last extension) for PGHS-1 and 32 (Day 8) or 40 (Day 12) cycles (94° C, 15 seconds; 60° C, 15 seconds; 72° C, 1 minute, 7 minutes for the last extension) for PGHS-2 mRNA measurements, using the following primers—antisense PGHS-1: 5'-aatctgactttctgagttgcc; PGHS-2: 5'-ttcagggagaagcgtttgc;

sense PGHS-1: 5'-5'-aggagatggctgctgagttgg; and PGHS-2: 5'-acacactctatcactggcacc. The resulting PCR products were 602 bp for endogenous PGHS-1 mRNA, 437 bp for PGHS-1 cRNA internal standard, 274 bp for endogenous PGHS-2 mRNA, and 143 bp for PGHS-2 cRNA internal standard. PCR products (15 μl) were separated on 1.8% agarose gels containing ethidium bromide (0.5 g/ml). Gels were photographed on a UV transilluminator, and images were scanned into a desktop computer. Densitometric analysis was done using ImageQuant software (Molecular Dynamics, Sunnyvale, California). The relative amounts of PGHS mRNA in each sample were calculated as mRNA/cRNA densitometric ratios.

Acknowledgements

References

Ballou LR, Botting RM, Goorha S, Zhang J, and Vane JR (2000). Nociception in cyclooxygenase isozyme-deficient mice. Proc Natl Acad Sci USA 97:10272–10276.

Boyle JE, Lindroos PM, Rice AB, Zhang L, Zeldin DC, and Bonner JC (1999). Prostaglandin-E_2 counteracts interleukin-1beta-stimulated upregulation of platelet-derived growth factor-receptor on rat pulmonary myofibroblasts. Am J Respir Cell Mol Biol 20:433–440.

Brzozowski T, Konturek SJ, Majka J, Dembinski A, and Drozdowicz D (1993). Epidermal growth factor, polyamines, and prostaglandins in healing of stress-induced gastric lesions in rats. Dig Dis Sci 38:276–283.

Castano E, Bartrons R, and Gil J (2000). Inhibition of cyclooxygenase-2 decreases DNA synthesis induced by platelet-derived growth factor in Swiss 3T3 fibroblasts. J Pharmacol Exp Ther 293:509–513.

Daniel TO, Liu H, Morrow JD, Crews BC, and Marnett LJ (1999). Thromboxane A_2 is a mediator of cyclooxygenase-2-dependent endothelial migration and angiogenesis. Cancer Res 59:4574–4577.

Dinchuk JE, Car BD, Focht RJ, Johnston JJ, Jaffee BD, Covington MB, Contel NR, Eng VM, Collins RJ, Czerniak PM, Gorry SA, and Trzaskos JM (1995). Renal abnormalities and an altered inflammatory response in mice lacking cyclooxygenase II. Nature 378:406–409.

Dong YL, Fleming RY, Yan TZ, Herndon DN, and Waymack JP (1993). Effect of ibuprofen on the inflammatory response to surgical wounds. J Trauma 35:340–343.

Fang C, Alexander JW, MacMillan BG, and Austin LS (1983). Failure of topical prostaglandin inhibitors to improve wound healing following deep partial-thickness burns. J Trauma 23:300–304.

Gonul B, Soylemezoglu T, Yanicoglu L, and Guvendik G (1993). Effects of epidermal growth factor on serum zinc and plasma prostaglandin E_2 levels of mice with pressure sores. Prostaglandins 45:153–157.

Hirose Y, Goto H, Arisawa T, Hase S, Niwa Y, Hayakawa T, Asai J, and Tsukamoto Y (1997). Kinetics of fibroblasts in ulcer healing in rats: Interference with indomethacin. Digestion 58:332–339.

Kirtikara, K, Morham SG, Raghow, R, Laulederkind SJF, Kanekura, K, Goorha S, and Ballou LR (1998). Compensatory prostaglandin E2 biosynthesis in cyclooxygenase 1 or 2 null cells. J Exp Med 187:517–523.

Langenbach R, Morham SG, Tiano HF, Loftin CD, Ghanayem BI, Chulada PC, Mahler JF, Lee CA, Goulding EH, Kluckman KD, and Smithies O (1995). Prostaglandin synthase 1 gene disruption in mice reduces arachidonic acid-induced inflammation and indomethacin-induced gastric ulceration. Cell 83:483–492.

LeDuc LE, Su KC, Guth E, Reedy T, and Guth PH (1993). Effects of cyclooxygenase and lipoxygenase inhibition on eicosanoids and healing of acetic acid colitis in rats. Dig Dis Sci 38:289–294.

Martinez-Hernandez A (1996). Repair and regeneration. In: Damjanov I and Linder J, eds. Anderson's pathology. St. Louis: Mosby, 416–447.

Mast B (1992). The skin. In: Cohen I, Diegelmann R, and Lindblad W, editors. Wound healing. Philadelphia: WB Saunders, 344–355.

Moreno JJ (1997). Regulation of arachidonic acid release and prostaglandin formation by cell-cell adhesive interaction in wound repair. Pflugers Arch 433:351–356.

Moreno JJ (2000). Resveratrol modulates arachidonic acid release, prostaglandin synthesis, and 3T6 fibroblast growth. J Pharmacol Exp Ther 294:333–338.

Morham SG, Langenbach R, Loftin CD, Tiano HF, Vouloumanos N, Jennette JC, Mahler JF, Kluckman KD, Ledford A, Lee CA, and Smithies O (1995). Prostaglandin synthase 2 gene disruption causes severe renal pathology in the mouse. Cell 83:473–482.

Nie D, Lamberti M, Zacharek A, Li L, Szekeres K, Tang K, Chen Y, and Honn KV (2000). Thromboxane A(2) regulation of endothelial cell migration, angiogenesis, and tumor metastasis. Biochem Biophys Res Commun 267:245–251.

Raghow R (1994). The role of extracellular matrix in postinflammatory wound healing and fibrosis. FASEB J 8:823–831.

Sanchez T and Moreno JJ (2001). Role of phospholipase A(2) in growth-dependent changes in prostaglandin release from 3T3 fibroblasts. J Cell Physiol 189:237–243.

Schilling JA (1976). Wound healing. Surg Clin North Am 56:859–874.

Schumacher HR Jr, editor (1988). Primer on the rheumatic diseases, 9th ed. Atlanta: Arthritis Foundation.

Smith WL and Langenbach R (2001). Why there are two cyclooxygenase isozymes? J Clin Invest 107:1491–1495.

Sun WH, Tsuji S, Tsujii M, Gunawan ES, Sawaoka H, Kawai N, Iijima H, Kimura A, Kakiuchi Y, Yasumaru M, Sasaki Y, Kawano S, and Hori M (2000). Cyclo-oxygenase-2 inhibitors suppress epithelial cell kinetics and delay gastric wound healing in rats. J Gastroenterol Hepatol 15:752–761.

Talwar M, Moyana TN, Bharadwaj B, and Tan LK (1996). The effect of a synthetic analogue of prostaglandin E_2 on wound healing in rats. Ann Clin Lab Sci 26:451–457.

Tsujii M, Kawano S, Tsuji S, Sawaoka H, Hori M, and DuBois RN (1998). Cyclooxygenase regulates angiogenesis induced by colon cancer cells [published erratum appears in Cell 1998 Jul 24;94(2):following 271]. Cell 93:705–716.

Zhang J, Goorha, S, Raghow, R, and Ballou LR (In press, 2002). The tissue-specific, compensatory expression of reciprocal cyclooxygenase isozymes in transgenic mice. Prostaglandins Other Lipid Mediat.

Zhang K, Rekhter MD, Gordon D, and Phan SH (1994). Myofibroblasts and their role in lung collagen gene expression during pulmonary fibrosis: A combined immunohistochemical and in situ hybridization study. Am J Pathol 145: 114–125.